

# Functional Regression Models with Functional Response: New Approaches and a Comparative Study

Mohammad Darbalaei<sup>\*1,2</sup>, Morteza Amini<sup>†1</sup>, Manuel Febrero-Bande<sup>‡2</sup>, and Manuel Oviedo-de la Fuente<sup>§3</sup>

<sup>1</sup>Dpt. of Statistics, School of Mathematics, Statistics and Computer Science, University of Tehran, Tehran, Iran

<sup>2</sup>Dpt. of Statistics, Mathematical Analysis and Optimization, Univ. de Santiago de Compostela, Santiago de Compostela, Spain

<sup>3</sup>Dpt. of Mathematics, CITIC, Univ. de A Coruña, A Coruña, Spain

July 12, 2022

## Abstract

This paper proposes three new approaches for additive functional regression models with functional responses. The first one is a reformulation of the linear regression model, and the last two are on the yet scarce case of additive nonlinear functional regression models. Both proposals are based on extensions of similar models for scalar responses. One our nonlinear model is based on constructing a Spectral Additive Model (the word “Spectral” refers to the representation of the covariates in a  $\mathcal{L}_2$  basis), which is restricted (by construction) to Hilbertian spaces. The other one extends the kernel estimator, and it can be applied to general metric spaces since it is only based on distances. We include our new approaches as well as real datasets in an R package. The performances of the new proposals are compared with previous ones, which we review theoretically and practically in this paper. The simulation results show the advantages of the nonlinear proposals and the small loss of efficiency when the simulation scenario is truly linear. Finally, the supplementary material provides a visualization tool for checking the linearity of the relationship between a single covariate and the response.

**Keywords:** Functional data analysis, Functional regression, Functional response, Linear and nonlinear models.

**Mathematics Subject Classification:** 62R10, 62–04, 62G08, 62J02

---

<sup>\*</sup>mohammad.darbalaei@rai.usc.es

<sup>†</sup>Corresponding author, e-mail: morteza.amini@ut.ac.ir

<sup>‡</sup>manuel.febrero@usc.es

<sup>§</sup>manuel.oviedo@udc.es

# 1 Introduction

Since the seminal book of [Ramsay and Silverman \(2005\)](#), Functional Data Analysis (FDA) has become an important field in Statistics. The term FDA is reserved for discussing random functions, surfaces or volumes. In its primary definition, FDA deals with data consisting of curves with a common domain, typically a fixed interval  $\mathcal{S} = [a, b]$  ( $\mathcal{S} = [0, 1]$  without loss of generality). These curves are usually assumed to belong to the Hilbert space  $\mathcal{L}_2(\mathcal{S}) := \{f : \mathcal{S} \rightarrow \mathbb{R} \text{ st } \int_{\mathcal{S}} |f(s)|^2 ds < \infty\}$ , equipped with an inner product, defined as:  $\langle f, g \rangle := \int_{\mathcal{S}} f(s)g(s)ds$ , its corresponding norm  $\|f\|_2 := \sqrt{\langle f, f \rangle}$  and the associated metric/distance among elements:  $d_2(f, g) := \|f - g\|_2$ . In practice, the curves are usually observed in a grid  $a = t_1 < t_2 < \dots < t_{r_{\mathcal{S}}} = b \in \mathcal{S}$  which might be dense or sparse, depending on measuring situations.

The key difference between FDA and multivariate data analysis (MV) is the dimension of the objects involved and hence, the dimension of the space. The observations in MV belong to Euclidean spaces,  $\mathbb{R}^p$ , whereas FDA is usually reserved for talking about statistical objects like functions, images or surfaces, which are of infinite dimension. A couple of big differences can be drawn from the infinite dimension of functional spaces. First, the objects of the space cannot be completely represented; thus, a dimension reduction tool must be performed when possible. Second, usual tricks in MV are now invalid in FDA due to the functional nature of the spaces. For instance, in a dense grid, the values of the curves at neighboring grid points become more and more interdependent, and an attempt to compute the inverse of the covariance matrix of the data become an ill-posed problem. The third main difference is that the common definitions of density and distribution function cannot be used for functional random elements due to the infinite dimension of the functional space. As a competitor of the MV, FDA has found its own path to solve these difficulties and even has evolved to deal with other kinds of functional spaces like Banach or metric (see, for instance, [Ferraty and Vieu \(2006\)](#)) or with more complex objects (see, for instance, [Locantore et al. \(1999\)](#)). A Banach space is a complete vector space equipped with a norm which does not necessarily have an inner product. A Hilbert space is always a Banach space with the associated norm  $\|f\| = \sqrt{\langle f, f \rangle}$ . However, the reverse is not true in general since it is impossible to define an inner product operator associated to a particular norm. Also, every Banach space is a metric space to the associated metric  $d(f, g) := \|f - g\|$  and, again, the reverse is not generally true.

FDA has developed many techniques for functional data including outlier detection, clustering, classification, time series and regression. A Functional Regression Model (FRM) is a regression model in which the response and/or any covariates belong to a functional space. The FRM models can be categorized depending on the type of the response and the covariates (functional or scalar), and the relationship between them (linear or nonlinear). The best-known functional regression problem in the literature is the functional linear regression with a scalar response, sometimes referred to as the linear scalar-on-function model. In this model, the functional covariate  $\mathcal{X}$  is assumed to belong to  $\mathcal{L}_2(\mathcal{S})$ , and the linear relation is modeled by the usual integral linear operator  $\int_{\mathcal{S}} \mathcal{X}(t)\beta(t)dt$ , where  $\beta \in \mathcal{L}_2(\mathcal{S})$  is an unknown coefficient function. The

key idea for estimating this model is to represent  $\beta$  and/or  $\mathcal{X}$  on an  $\mathcal{L}_2$  basis. This basis could be a fixed basis like Fourier or a B-spline basis (see, for instance, (Ramsay and Silverman, 2005, Chap. 5), Cardot et al. (2003), Cardot et al. (2007) or James et al. (2009)) or a data-driven basis like functional Principal Components (fPC) or functional Partial Least Squares (fPLS) (see Cardot et al. (1999), Preda and Saporta (2005), Reiss and Ogden (2007), Hall et al. (2006), Delaigle et al. (2012) or Febrero-Bande et al. (2017) among many others). In a nonlinear FRM, the assumption of having a linear operator is relaxed, and the relationship between the response and covariates is assumed to be an unknown general operator. Indeed, in these models, one can even relax the assumption that the functional variables belong to the Hilbert space. For the estimation of the unknown operator, different methods are proposed in the literature, including the kernel approaches (see, for instance, Ferraty and Vieu (2006), Aneiros-Pérez and Vieu (2006), Ferraty and Vieu (2009) or Febrero-Bande and González-Manteiga (2013)) or by transforming the link among the covariate(s) and the response (see Müller and Yao (2008), Ferraty et al. (2013), Chen et al. (2011), McLean et al. (2014) or Fan and James (2011)). The case when both the response and the covariate(s) are functional (aka function-on-function regression) has attracted much less attention in the literature. For the linear case, see, for instance, (Ramsay and Silverman, 2005, Chap. 16), Cuevas et al. (2002), Chiou et al. (2003), Ivanescu et al. (2014), Chiou et al. (2016) or Beyaztas and Shang (2020). The nonlinear case is more scarce with Ferraty et al. (2012b) devoted to kernel approaches and Scheipl et al. (2015) and Qi and Luo (2019), where the chosen approach includes spline-based and fPC-based terms.

This paper focuses on the yet scarce case of nonlinear functional regression models with functional responses that can accommodate more than one functional covariate in the model. We propose three novel approaches; one deals with linear and two deal with nonlinear regression models. For linear models, we represent all covariates, the response and the coefficient functions on appropriate bases. The model is flexible enough to incorporate a variety of basis expansions such as PC, PLS, and splines. We also extend the results of Febrero-Bande et al. (2017) for scalar response for computing the conditional mean-square prediction error, for a new observation, to the case of functional response. The presented formula is simplified in the particular case of considering PC basis for representing covariates and the response. For nonlinear cases, we have extended the spectral additive method proposed by Müller and Yao (2008) to the case of functional response. To enter the participation of each covariate, they use a combination of smooth functions over the coefficients derived by a basis representation of the covariate. The kernel additive method is another novel approach for estimating nonlinear operator(s) in additive functional regression models with functional responses. The main advantage of this method is that the assumption that the response and all the covariates belong to Hilbert space is relaxed. To the best of our knowledge, all the available approaches in the literature only focus on smooth models. Our proposal, however, is the first publicly available implementation of both smooth and non-smooth models in the scope of functional response. In addition, different nonlinear methods are studied and compared with each other and the usual linear FRMs through several

simulation scenarios and several real datasets. The examples will show the advantages of the nonlinear proposals and the small loss of efficiency when the scenario is truly linear. Furthermore, we present some graphical tools and visualization methods to assess the assumption of linearity or nonlinearity of the regression operator (in the supplementary material).

The structure of the paper is as follows. Section 2 introduces the framework of functional regression models with functional responses. Section 3 provides the inference procedure for the proposed linear approach. Section 4 is devoted to the developed approaches for estimating nonlinear operators as well as an overview of some nonlinear methods in the FDA literature. Section 5 provides the practical advice for applying these models and contains the simulation studies. Finally, two applications to real data are provided in Section 6. A graphical tool for assessing the assumption of linearity of the regression operator is presented in the supplementary material. The proposed methods are all included in a recently updated version of the `fda.usc` R package.

## 2 Functional Regression Models with Functional Response

Let  $\{\mathcal{Y}, \{\mathcal{X}^1, \dots, \mathcal{X}^J\}\}$  be a vector of functional elements in the product space  $\mathcal{F}_{\mathcal{Y}} \times \mathcal{F}_{\mathcal{X}^1} \times \dots \times \mathcal{F}_{\mathcal{X}^J}$ , where each  $\mathcal{F}_{\bullet}$  is a normed functional space whose elements are measurable continuous functions almost everywhere, with domains  $\{\mathcal{S}_{\mathcal{Y}}, \mathcal{S}_1, \dots, \mathcal{S}_J\}$ , i.e.  $\mathcal{F}_{\bullet} := \{f : \mathcal{S}_{\bullet} \rightarrow \mathbb{R} \text{ st } \int_{\mathcal{S}_{\bullet}} |f(t)|^p dt < \infty\}$ , where  $1 \leq p < \infty$ . These spaces are the so-called *Lebesgue Spaces* that are all normed spaces with the norm  $\|f\|_p = \left( \int_{\mathcal{S}_{\bullet}} |f(t)|^p dt \right)^{1/p}$ .

The general case of a Functional Regression Model with Functional Response (FRMFR) is given by

$$\mathcal{Y} = \alpha + m(\mathcal{X}^1, \dots, \mathcal{X}^J) + \epsilon, \quad (1)$$

where  $m : \mathcal{F}_{\mathcal{X}^1} \times \dots \times \mathcal{F}_{\mathcal{X}^J} \rightarrow \mathcal{F}_{\mathcal{Y}}$  is the regression operator among covariate spaces and the response space and  $\{\alpha, \epsilon\} \in \mathcal{F}_{\mathcal{Y}}$  with  $\mathbb{E}[\epsilon] = 0$ . For identifiability purposes and without loss of generality, we can assume that all covariates are centered. Thus,  $\mathbb{E}[m(\cdot)] = 0$  and  $\alpha := \mathbb{E}[\mathcal{Y}]$ . The second common hypothesis in regression models is that  $\epsilon$  and the covariates are independent, i.e.  $\text{Cov}(\mathcal{X}^j(s), \epsilon(t)) = 0 \forall s, t \in \mathcal{S}_j \times \mathcal{S}_{\mathcal{Y}}, \forall j = 1, \dots, J$ .

The task of identifying and estimating the operator  $m$  in Model (1) is quite challenging, not only due to the effect of the so-called curse of dimensionality but also due to the complexity of the statistical objects involved. In the following sections, we will consider different models for estimating the operator  $m(\cdot)$  that provide different ways of predicting the functional response. The construction of these different models must consider the characteristics of the functional spaces where the covariates and the response live and the properties of the model itself.

The next step (not covered in this work) is to extend the Functional Regression Models to estimate Functional Time Series (FTS) using a similar framework. For instance, considering a sequence

$$(\mathcal{Z}_1, \mathcal{W}_1^1, \dots, \mathcal{W}_1^q), \dots, (\mathcal{Z}_n, \mathcal{W}_n^1, \dots, \mathcal{W}_n^q)$$

of elements in the functional space  $\mathcal{F}_{\mathcal{Z}} \times \mathcal{F}_{\mathcal{W}^1} \times \cdots \times \mathcal{F}_{\mathcal{W}^q}$  are denoted by  $\mathcal{Y}_l = \mathcal{Z}_l$  and  $\mathcal{X}_l^j = \mathcal{Z}_{l-j}$ ,  $j = 1, \dots, p$  and by,  $\mathcal{X}_l^j = \mathcal{W}_l^{j-p}$ ,  $j = p+1, \dots, p+q$ ,  $l = p+1, \dots, n$ . Then, a Functional Additive Model can be written as

$$\mathcal{Z}_l = \alpha + \sum_{j=1}^p \Phi_j(\mathcal{Z}_{l-j}) + \sum_{j=p+1}^{p+q} \Phi_j(\mathcal{W}_l^{j-p}) + \epsilon_l, \quad l = p+1, \dots, n$$

which is also named as a Functional Auto-Regressive Model with  $q$  exogenous covariates (FARX). Suppose no exogenous information is available and all  $\Phi$ 's are linear. In that case, we have a Functional Linear Auto-Regressive Model of order  $p$  (FLAR( $p$ )), also known as a Hilbertian AR (ARH( $p$ )). Of course, treating of an FTS as an FRMFR requires adding additional assumptions to parameters and covariates to ensure, for instance, stationarity and new tools for testing or capturing the temporal characteristics of the FTS.

### 3 Functional Linear Models

The Functional Linear Model with Functional Response (FLMFR) is defined as follows

$$\mathcal{Y}(t) = \alpha(t) + \sum_{j=1}^J \langle \mathcal{X}^j, \beta_j \rangle(t) + \epsilon(t), \quad (2)$$

where  $\langle \mathcal{X}^j, \beta_j \rangle(t) := \int_{\mathcal{S}_j} \mathcal{X}^j(s) \beta_j(s, t) ds$  with  $\beta_j \in \mathcal{F}_{\mathcal{X}^j} \times \mathcal{F}_{\mathcal{Y}}$ ,  $\alpha \in \mathcal{F}_{\mathcal{Y}}$  and  $\epsilon \in \mathcal{F}_{\mathcal{Y}}$  is a zero mean process with covariance function  $\text{Cov}(\epsilon(t'), \epsilon(t)) = \Sigma_{\epsilon}(t', t)$ . Without loss of generality, all covariates and the response can be centered and then  $\alpha \equiv 0$ . As in the multivariate case,  $\alpha$  can be estimated for non-centered variates as  $\hat{\alpha} = \bar{\mathcal{Y}} - \sum_{j=1}^J \langle \bar{\mathcal{X}}^j, \hat{\beta}_j \rangle$ .

For the sake of simplicity, let us consider the linear model with just one covariate  $\mathcal{X}$  in the following. The key idea is to take advantage of the Hilbert structure for representing the response, the parameter  $\beta$  and the covariate on an appropriate basis and approximate the Functional Regression problem by a Multivariate Linear Model.

Be explicit and consider that we can approximately represent  $\mathcal{Y}$  in a basis  $\theta$  with  $L$  elements,  $\mathcal{X}$  in a basis  $\eta$  with  $K$  elements, and  $\beta_1$  in a tensor product basis  $(\eta^*, \theta^*)$  with  $(K^*, L^*)$ <sup>1</sup>. The functions are observed in grids  $t_1, \dots, t_{r_T} \in \mathcal{S}_{\mathcal{Y}}$  and  $s_1, \dots, s_{r_S} \in \mathcal{S}_{\mathcal{X}^1}$ , respectively. Then, the function evaluations over the grids and their approximate basis representations can be written in the following matrix forms:

---

<sup>1</sup>The usual choice is to let  $\eta^* = \eta$ ,  $\theta^* = \theta$ ,  $K^* = K$  and  $L^* = L$  to reduce computations.

$$\begin{aligned}
\mathcal{Y}_i(t_j) &\approx \sum_{l=1}^L y_{il}\theta_l(t_j), \quad i = 1, \dots, n, \quad j = 1, \dots, r_T \implies \mathbf{Y} \approx \mathbf{y}\boldsymbol{\theta} \\
\mathcal{X}_i(s_j) &\approx \sum_{k=1}^K x_{ik}\eta_k(s_j), \quad i = 1, \dots, n, \quad j = 1, \dots, r_S \implies \mathbf{X} \approx \mathbf{x}\boldsymbol{\eta} \\
\beta(s_i, t_j) &\approx \sum_{k=1}^{K^*} \sum_{l=1}^{L^*} b_{k,l}\eta_k^*(s)\theta_l^*(t) \quad i = 1, \dots, r_S, \quad j = 1, \dots, r_T \implies \boldsymbol{\beta} \approx \boldsymbol{\eta}^{*\top} \mathbf{B} \boldsymbol{\theta}^*
\end{aligned}$$

where  $\mathbf{x} = (x_i(s_j))_{i,j=1}^{n,r_S}$ ,  $\mathbf{y} = (y_i(t_j))_{i,j=1}^{n,r_T}$  are values at the grid points for  $\mathcal{X}$  and  $\mathcal{Y}$ , respectively,  $\mathbf{B} = (b_{kl})_{k,l=1}^{K^*,L^*}$  is the coefficient matrix for  $\beta$ . Also,  $\boldsymbol{\eta} = (\eta_k(s_j))_{k,j=1}^{K,r_S}$ ,  $\boldsymbol{\theta} = (\theta_l(t_j))_{l,j=1}^{L,r_T}$  (resp.  $\boldsymbol{\eta}^*$ ,  $\boldsymbol{\theta}^*$ ) are the evaluations of the tensor product basis on the double grid.

Similar to the multivariate case, Model (2) can be estimated by minimizing the Residual Sum of Squares Norms  $RSSN(\beta) = \sum_{i=1}^n \|\mathcal{Y}_i - \hat{\mathcal{Y}}_i\|^2$ , which is represented by

$$RSSN(\mathbf{B}) \approx \sum_{i=1}^n \|\epsilon_i\|^2 = \sum_{i=1}^n \|\mathbf{y}_i \boldsymbol{\theta} - \mathbf{x}_i \boldsymbol{\eta} \boldsymbol{\eta}^{*\top} \mathbf{B} \boldsymbol{\theta}^*\|^2.$$

Using this trick, the estimation of  $\boldsymbol{\beta}$  relies on finding the  $K^* \times L^*$  parameters of  $\mathbf{B}$  instead of the  $r_S \times r_T$  parameters of  $\boldsymbol{\beta}$ . Another advantage is that by choosing an appropriate basis (for instance, orthogonal), the dependence among columns of  $\mathbf{X}$  is no longer a big problem. Therefore, the two basis must be chosen such that their numerical properties are balanced with their representation quality. Note that the tensor product basis expansion of  $\beta$  might use different basis functions from those associated with  $\mathcal{X}$  and  $\mathcal{Y}$ . As pointed out by Preda and Schiltz (2011), a PLS basis has an equivalence between the functional model and the Multiple Linear Model among representation coefficients in the basis for the covariate and the response. That result can be extrapolated to any type of basis. Also, suppose some penalization on  $\boldsymbol{\eta}$  or  $\boldsymbol{\theta}$  (typically related to smoothing) is desired. In that case, an appropriate penalization matrix and factor can be added to  $RSSN(B)$ . For an introductory view on this, one can refer to (Ramsay and Silverman, 2005, Chap. 16). We extend the results of Febrero-Bande et al. (2017) to compute the conditional mean-square prediction error (CMSPE) of the scalar response for a new observation  $(\mathcal{Y}_0, \mathcal{X}_0)$  by considering the special case of  $K^* = K$ ,  $L^* = L$  and employing the PC basis  $\boldsymbol{\eta}^* = \boldsymbol{\eta}$  and  $\boldsymbol{\theta}^* = \boldsymbol{\theta}$ . Then, the following expression can be obtained for functional response case:

$$\mathbb{E} \left[ \left\| \mathcal{Y}_0 - \hat{\mathcal{Y}}_0 \right\|^2 | \mathcal{X} \right] = \sum_{l=1}^L \left( \hat{\sigma}_{(l)}^2 + \frac{\hat{\sigma}_{(l)}^2}{n} \left( 1 + \sum_{k=1}^K \frac{x_{0,l}^2}{\hat{\lambda}_k} \right) \right) + \|R_K^{\mathcal{X}}\|^2 + \|R_L^{\mathcal{Y}}\|^2,$$

where  $\mathcal{Y}_0 = \sum_{l=1}^{\infty} y_{0,l}\theta_l$ ,  $\hat{\mathcal{Y}}_0 = \sum_{l=1}^L \hat{y}_{0,l}\hat{\theta}_l$ ,  $R_L^{\mathcal{Y}} = \sum_{l=L+1}^{\infty} y_{0,l}\theta_l$ ,  $R_K^{\mathcal{X}} = \sum_{k=K+1}^{\infty} x_{0,k}\eta_k$ ,  $\hat{\lambda}_k$  is the estimation of  $k$ -th eigenvalue for  $\mathcal{X}$ , and

$$\hat{\sigma}_{(l)}^2 = \frac{1}{n-K} \sum_{i=1}^n \left( y_{il} - \sum_{k=1}^K \hat{b}_{kl} x_{ik} \right)^2.$$

Leaving aside the role of the two remainder representation terms,  $R_K^{\mathcal{X}}$  and  $R_L^{\mathcal{Y}}$ , which decrease as  $K$  and  $L$  increase, the play of these parameters is not symmetric. Although  $L$  has an impact only in the remaining term to obtain a better approximation,  $K$  can substantially effect the CMSPE depending on the values of the eigenvalues. Other effects of covariates in the CMSPE are related to  $\hat{\sigma}_{(l)}^2$ , which decreases as  $K$  increases. So, the choice of  $K$  seems more critical than the choice of  $L$  and must be balanced its effect among  $\hat{\sigma}_{(l)}^2$  and  $\hat{\lambda}_1, \dots, \hat{\lambda}_K$ .

Different approaches found in the literature differ essentially in the type of basis employed, the type of penalization and the type of numerical integration method. For instance, [Ivanescu et al. \(2014\)](#) use the Penalized Functional Regression (PFR) presented by [Goldsmith et al. \(2011\)](#), representing the covariates in a large number of eigenfunctions and the functional coefficient using a Penalized Spline Regression. The Linear Signal Compression approach (LSC) proposed by [Luo and Qi \(2017\)](#) represents the  $\beta$  coefficient using the eigenfunctions of the covariate as  $\boldsymbol{\eta}$  and the eigenfunctions of the response as  $\boldsymbol{\theta}$ . So,  $\beta$  is constructed as a tensor product basis expansion of the Karhunen–Loeve representations of  $\mathcal{X}$  and  $\mathcal{Y}$ .

The extension to multiple covariates of any of the above approaches is straightforward since the FLMFR is estimated through an approximation to a Multiple Linear Model among the coefficients of the representation of the covariates and the coefficients of the representation of the response. The main drawback of all these approaches is how to balance the parsimony of the model with the quality of the representation for covariates and response.

## 4 Functional Nonlinear Models

Two novel nonlinear functional regression models are proposed in the following two subsections. In the final subsection, other available nonlinear competitors are briefly described. All of them will be compared in the numerical study section.

### 4.1 Functional Spectral Additive Model

One way of considering more complex relationship than the linear model is to use the idea put forward by [Müller and Yao \(2008\)](#) for the case of a single functional covariate and a scalar response which, we call “Spectral Additive”. The key motivation of this method is that in a FLMFR, the expectation of the fPC scores of the functional response is a linear function of the fPC scores of the functional covariate. Thus, one way of extending the linear model is to consider additive nonlinear components of the fPC scores of the covariate. Suppose that  $\mathcal{X}^j$  has the following truncated basis representation

$$\mathcal{X}^j \approx \sum_{k=1}^{K_j} x_k^j \eta_k.$$

Then, the usual basis to represent  $\mathcal{X}^j$  is given by the fPC, which is the spectral representation of the covariance operator. For a scalar response, the Functional Spectral Additive Model (FSAM)

is defined as

$$y = \alpha + \sum_{j=1}^J \Phi_j(\mathcal{X}^j) + \epsilon = \alpha + \sum_{j=1}^J \sum_{k=1}^{K_j} f_{jk}(x_k^j) + \epsilon, \quad (3)$$

where  $f_{jk}$  is a general nonlinear function,  $x_k^j$  is the  $k^{\text{th}}$  coefficient of the basis for representing  $\mathcal{X}^j$  and fulfilling, for identifiability purposes, that  $\mathbb{E}[f_{jk}(x_k^j)] = 0 \ \forall j, k$ . Again, as before,  $\epsilon$  is a zero mean vector with covariance operator  $\Sigma_\epsilon$ . FLM is the particular case of this model when  $f_{jk}$  is linear. Using a basis representation, the additive model can only be applied to Hilbertian covariates. One of the advantages of additive models in the multivariate framework is that the contribution of each covariate can be easily interpreted. This advantage is diluted in the functional framework because the interpretation of the effects of a functional covariate must be done jointly considering the functions  $f_{jk}$  along with the basis and the estimated coefficients. Except in some simple cases, this can be a challenging task. On the other hand, choosing an orthogonal basis, the collinearity problem is minimized among functions associated with the same covariate.

The extension of Model (3) to functional response (FSAMFR) can be done in one of the following two strategies:

- Fitting Model (3) for each evaluations  $\mathcal{Y}(t_1), \dots, \mathcal{Y}(t_{r_T})$ , over the grid  $t_1, \dots, t_{r_T} \in \mathcal{S}_Y$ ,

$$\mathcal{Y}(t_l) = \alpha(t_l) + \sum_{j=1}^J \sum_{k=1}^{K_j} f_{jk}^{(t_l)}(x_k^j) + \epsilon(t_l), l = 1, \dots, r_T. \quad (4)$$

- Fitting Model (3) for each coefficients  $y_1, \dots, y_L$  of the basis representation  $\mathcal{Y} \approx \sum_{l=1}^L y_l \theta_l$ ,

$$y(l) = \alpha(l) + \sum_{j=1}^J \sum_{k=1}^{K_j} f_{jk}^{(l)}(x_k^j) + \epsilon(l), l = 1, \dots, L. \quad (5)$$

If the representation of the response is done on an orthogonal basis, the equations in Model (5) deal with uncorrelated responses and thus, we see only a small (or null) dependence among  $y(l)$  for  $l = 1, \dots, L$ . On the contrary, if the discretization grid is dense, the equations in Model (4) deal with high dependence among  $\mathcal{Y}(t_l)$  for  $l = 1, \dots, r_T$ . In that case, despite the fact, the way of estimating  $\mathcal{Y}(t_l)$  for  $l = 1, \dots, r_T$  does not work efficiently since the optimization for each  $t_l$  can lead to instabilities on the continuity of the estimator along the grid. Indeed, the loop should be done over a greater number of elements than in the previous case. Therefore, it seems that there is no main advantage of using Model (4) instead of Model (5). In Model(5), although there is no closed form for CMSPE, like in the linear case, it seems that their constructions are similar, the closed form should be similar to the linear case, but it may include some additional conditions over  $f_{jk}^{(l)}$ . In our experience, Model (5) has a certain overfitting tendency that can be controlled by imposing restrictions on the flexibility of  $f_{jk}^{(l)}$ , but it is not always clear how to set them.



## 4.2 Functional Kernel Additive Model

Another way of considering a nonlinear additive model is to extend the kernel estimator proposed by [Febrero-Bande and González-Manteiga \(2013\)](#) for scalar response to the case of functional response (FKAMFR). Specifically, the model can be simply written as

$$\mathcal{Y} = \alpha + \sum_{j=1}^J \Phi_j(\mathcal{X}^j) + \epsilon. \quad (6)$$

In this model, the functional spaces associated with the response ( $\mathcal{F}_{\mathcal{Y}}$ ) or the covariates ( $\mathcal{F}_{\mathcal{X}^j}$ ) could be a general metric space (of course, including  $\mathcal{L}_2$ ). The case with a single functional covariate ( $J = 1$ ) was studied in [Ferraty et al. \(2012a\)](#) where some convergence results were obtained. For  $J > 1$ , there are only proposals for scalar responses. For instance, in [Ferraty and Vieu \(2009\)](#), some boosting ideas were applied to estimate a functional kernel regression model with  $J > 1$  and some illustrations with  $J = 2$  were provided. Also, the aforementioned work by [Febrero-Bande and González-Manteiga \(2013\)](#) extends the backfitting algorithm for functional covariates in the context of generalized responses. Our proposal here is to extend the backfitting algorithm for a functional response.

**Backfitting for Functional Covariates and Response (BFFCFR)** In short, the backfitting algorithm (BF) is an iterative procedure for estimating a regression model where the optimization of each covariate contribution is done assuming that the rest are fixed and performing a loop across covariates and iterations until convergence. So, BF consists of two nested loops: the outer one is the overall iteration until convergence, and the inner one is the cycle across covariates. The BFFCFR algorithm is as follows

- Initialize the estimators with  $\hat{\alpha}^{(0)} := \bar{\mathcal{Y}}$  and  $\Phi_j^{(0)} := 0$  for  $j = 1, \dots, J$ .
- In the  $s^{\text{th}}$  iteration, update the current estimation of  $\Phi_j$  for  $j = 1, \dots, J$  by

$$\hat{\Phi}_j^{(s)}(\mathcal{X}_0^j) = \frac{\sum_{i=1}^n \left( \mathcal{Y}_i - \hat{\mathcal{Y}}_i^{(-j)} \right) K_j \left( \frac{d_j(\mathcal{X}_0^j, \mathcal{X}_i^j)}{h_j} \right)}{\sum_{m=1}^n K_j \left( \frac{d_j(\mathcal{X}_0^j, \mathcal{X}_m^j)}{h_j} \right)}, \quad (7)$$

where

$$\hat{\mathcal{Y}}_i^{(-j)} = \hat{\alpha}^{(s)} + \sum_{k=1}^{j-1} \hat{\Phi}_k^{(s)}(\mathcal{X}_i^k) + \sum_{k=j+1}^J \hat{\Phi}_k^{(s-1)}(\mathcal{X}_i^k),$$

$K_j$  is a suitable kernel function,  $h_j > 0$  is a proper bandwidth and  $d_j : \mathcal{F}_{\mathcal{X}^j} \times \mathcal{F}_{\mathcal{X}^j} \rightarrow \mathbb{R}^+$  is the metric or semi-metric associated with the norm of the functional space  $\mathcal{S}_{\mathcal{X}^j}$ .

- Repeat iterations until convergence:  $\|\Phi_j^{(s)} - \Phi_j^{(s-1)}\| < \delta, \forall j = 1, \dots, J$ .

The final prediction after  $s$  iterations is given by

$$\hat{\mathcal{Y}}_0 = \bar{\mathcal{Y}} + \sum_{j=1}^J \hat{\Phi}_j^{(s)}(\mathcal{X}_0^j).$$

The optimization step made in Model (7) is computing a weighted mean of the pseudoresponses (the response minus the contribution of the other covariates) depending on the bandwidth parameter  $h_j$ . This parameter must be optimized by minimizing an appropriate loss function, typically related to the sum of the squared difference norms  $\min_{\mathbf{h}} \sum_{i=1}^n \|\mathcal{Y}_i - \hat{\mathcal{Y}}_i\|_{\mathcal{Y}}^2$ . This method can be applied to more general spaces than the Hilbert space. Note that  $\mathcal{F}_{\mathcal{Y}}$  must have a real vector space structure, in which Model (7) can be computed. A normed space always fulfils this condition, but this is not true for a general metric space. Also, depending on the metrics of the covariates, the optimization step can be more or less affordable. However, if  $h_j$  is a scalar parameter, an exhaustive search along a grid of values is always possible.

For the specific case when the functional response belongs to the Hilbert space, a possible alternative approach is to extend Model (6) by fitting Functional Kernel Additive Models with Scalar Response to each of the coefficients of an appropriate basis representation of the functional response (as was done in Model (5)) or to the evaluations of the response function on the grid points (as was done in Model (4)). Again, the latter seems unable to guarantee certain homogeneity through estimation procedure along the grid. For instance, the optimal value for the bandwidth could change for consecutive grid points. Fitting Functional Kernel Additive Models with Scalar Response to each of the coefficients of an orthogonal basis representation of the functional response seems to be a better choice for computation of Model (6), especially for sparse measurement of the response.

The properties of this model, including existence and convergence rates, can be deduced from Jeon et al. (2021), where an approach using the Smooth Backfitting (SBF) algorithm is employed for Hilbertian response variables and covariates in Hilbertian and semi-metric spaces or Riemannian manifolds. As in the multivariate framework, using SBF typically ensures the convergence of each  $\hat{\Phi}_k$  to  $\Phi_k$ , whereas the BF only ensures the global convergence of  $\hat{\mathcal{Y}}_0$  to  $\mathcal{Y}_0$ . The better properties of SBF are obtained at the cost of computing marginal densities for  $(\mathcal{X}^{(j)}, \mathcal{X}^{(k)})$  and  $\mathcal{X}^{(j)}$ , which can be problematic for infinite-dimensional spaces (Jeon et al. (2021) solved this by imposing that  $\mathcal{X}^{(j)}$  is a compact subset of  $q_j$ -dimensional Hilbert spaces or finite dimensional Riemannian manifolds).

### 4.3 Other Nonlinear Approaches

Some other nonlinear methods for regression models with functional response are described in the FDA literature with certain similarities with the above described. The approach by Scheipl et al. (2015), called Functional Additive Mixed Model (FAMM), is similar to Model (6) or Model (4) in the sense that an additive model is constructed for each grid point of the response being the covariates of different nature (scalar, functional, categorical, etc.). Focusing on functional

covariates, the FAMM is constructed as

$$\mathcal{Y}(t) = \alpha(t) + \sum_{j=1}^J f_j(\mathcal{X}^{(j)}, t) + \epsilon(t),$$

where  $\epsilon(t)$  is an i.i.d. gaussian noise with variance  $\sigma_\epsilon^2$ . This latter assumption is unreasonable for a functional framework in a Hilbert space with a dense grid. The reason is that any independent process along  $t$  does not belong to a Hilbert space as it is discontinuous almost everywhere ( $\lim_{t \rightarrow t_0} \epsilon(t) \neq \epsilon(t_0)$ ). This assumption is only acceptable when the grid is sparse and the gap among consecutive grid points is large enough to consider that the dependence has vanished.

The  $f_j$  function for functional effects can add a linear or nonlinear contribution to the model. In the linear case,  $f_j(\mathcal{X}^{(j)}, t) := \int_{S_j} \mathcal{X}^{(j)}(s) \beta_j(s, t) ds$  (similar to Model (2)), which might be estimated using a B-spline basis for representing  $\mathcal{X}^{(j)}$  and  $\beta_j$ . In the nonlinear case, one might consider  $f_j(\mathcal{X}^{(j)}, t) := \int_{S_j} F_j(\mathcal{X}^{(j)}(s), s, t) ds = \int_{S_j} F_{X,s}^j(x(s), s) F_t(t) ds$ , which also can be treated using B-spline expansions for  $F_{X,s}^j$  (bivariate) and  $F_t$ . Typically, a smoothness penalty term is added to the estimation of the model to avoid, particularly in the latter case, the inflation in the number of parameters.

An alternative idea for the nonlinear approach is provided by [Qi and Luo \(2019\)](#) who assumed

$$F_j(\mathcal{X}^{(j)}(s), s, t) = \sum_{k=1}^{\infty} G_k(\mathcal{X}^{(j)}(s), s) \phi_k(t),$$

which is called *Decomposition Induced by the Signal Compression* (DISC). The goal of this proposal is to find the partial  $\sum_{k=1}^K G_k(\mathcal{X}^{(j)}(s), s) \phi_k(t)$  with the minimum prediction error among all equivalent expansions of  $F_j$ . This can be done in two steps: (i) obtaining  $\hat{G}_k$  by solving a generalized eigenvalue problem with a smoothness penalty derived from a Sobolev norm, and (ii) estimating  $\phi_k$  given  $\hat{G}_k$ . Also, in practice  $\hat{G}_k$  is estimated using a tensor product B-spline basis, which induces more smoothness in the final estimator.

The main drawback of these approaches, apart from the high number of parameters, is how to generate the basis expansion of  $G_k$  at  $\mathcal{X}^{(j)}$ . The tensor product B-spline basis associated with values  $\mathcal{X}^{(j)}(s)$  must be constructed using the training sample. The values of these bases for new (future) curves may exceed the interval of the training sample, and this may produce a wiggly prediction for this new observation. Besides, if an outlier exists among the training sample, the range for the B-spline expansion could be distorted. In such a situation, the location of the knots (and so, the elements of the basis associated with them) may not be informative, which results in a considerable bias of final estimator. However, there is no problem with the basis expansion at points  $s$  or  $t$  since the intervals of these values are fixed.

## 5 Numerical Studies

This section compares our proposed methods (namely, FLMFR, FSAMFR, and FKAMFR, which are available in the `fda.usc` package through the commands `fregre.lm.fr`, `fregre.sam.fr`

and `fregre.kam.fr`) with the four mentioned competitor methods (namely, PFR, FMM, LSC, and DISC). PFR and FMM methods are available in the `refund` package through the command `pffr`, where the argument `formula` allows us to include linear `ffpc`, `ff` or nonlinear term `sff`. The authors considered the latter as an experimental feature. LSC and DISC methods are available in the `FRegSigCom` package through the commands `cv.sigcom` and `cv.nonlinear`. However, this package is not currently maintained; its latest version was published in November 2018. Note that in this comparison, FLMFR, PFR, and LSC are linear, while FSAMFR, FKAMFR, FMM and DISC are nonlinear methods. In all estimation cases when a basis is needed, we have chosen a principal component basis for each covariate or response with a length that ensures the percentage of variability explained (PVE) by the basis is over 95%.

For each simulation scenario, a training sample  $(\vec{\mathcal{X}}_i, \mathcal{Y}_i)_{i=1}^n$  with size  $n \in \{100, 200\}$  is generated, which is used for training all models. A prediction (validation) set  $(\vec{\mathcal{X}}_i^p, \mathcal{Y}_i^p)_{i=1}^{n_p}$  with size  $n_p = 100$  is also generated to examine the quality of the estimates out of the training sample. The simulation scenarios will be generated by fixing  $\rho^2$  defined as

$$\rho^2 = 1 - \frac{\mathbb{E} [\|\epsilon\|^2]}{\mathbb{E} [\|\mathcal{Y} - \mu_{\mathcal{Y}}\|^2]}.$$

Therefore, the methods will be compared using empirical measures of it

$$R_e^2 = 1 - \frac{\sum_{i=1}^n \|\mathcal{Y}_i - \hat{\mathcal{Y}}_i\|^2}{\sum_{i=1}^n \|\mathcal{Y}_i - \bar{\mathcal{Y}}\|^2},$$

$$R_p^2 = 1 - \frac{\sum_{i=1}^{n_p} \|\mathcal{Y}_i^p - \hat{\mathcal{Y}}_i^p\|^2}{\sum_{i=1}^{n_p} \|\mathcal{Y}_i^p - \bar{\mathcal{Y}}\|^2},$$

where  $\hat{\mathcal{Y}}_i, \hat{\mathcal{Y}}_i^p$  are the estimates over the training and the validation set, respectively.

## 5.1 Simulation Study

Eight scenarios were constructed to compare methods: four linear and four nonlinear. Also, in four scenarios the response depends only on the first covariate and in the rest, the response is generated using the two functional covariates. The first covariate ( $\mathcal{X}^{(1)}$ ) is generated from a zero-mean Ornstein-Uhlenbeck process in  $[0, 1]$ , with the following covariance function

$$\Sigma_1(u, v) = \frac{\sigma^2}{2\theta_1} \exp \left\{ -\theta_1(u + v) \right\} \left( \exp \{2\theta_1 \min(u, v)\} - 1 \right).$$

Here, we let  $\sigma = 1$  and  $\theta_1 = 0.2$ . The second covariate ( $\mathcal{X}^{(2)}$ ) is generated from a zero-mean Gaussian process with the following covariance function

$$\Sigma_2(u, v) = \sigma^2 \exp \left( \frac{-|u - v|}{\theta_2} \right). \quad (8)$$

In this case, we set  $\sigma^2 = 0.5$  and  $\theta_2 = 0.7$ . Both covariates were generated on an equi-spaced grid of 51 points. The rule  $\text{PVE} > 95\%$  applied to the covariates leads to select four PCs for  $\mathcal{X}^{(1)}$  and five for  $\mathcal{X}^{(2)}$ .

We used the following four scenarios to generate the functional response.

- Linear smooth (LS): The regression model is

$$\mathcal{Y} = \Delta \left( \langle \mathcal{X}^{(1)}, \beta_1^{\text{LS}} \rangle + \langle \mathcal{X}^{(2)}, \beta_2^{\text{LS}} \rangle \right) + \epsilon,$$

with constant  $\Delta$  and the following coefficient functions

$$\beta_1^{\text{LS}}(u, v) = 6\sqrt{uv} \sin(4\pi v)$$

and

$$\beta_2^{\text{LS}}(u, v) = -(uv + 1) \cos(2\pi\sqrt{uv}).$$

- Linear non-smooth (LNS): The regression model is

$$\mathcal{Y} = \Delta \left( \langle \mathcal{X}^{(1)}, \beta_1^{\text{LNS}} \rangle + \langle \mathcal{X}^{(2)}, \beta_2^{\text{LNS}} \rangle \right) + \epsilon,$$

with the following coefficient functions

$$\beta_1^{\text{LNS}}(u, v) = \begin{cases} 5.6 \exp(u^3) \left( \frac{v-0.1}{0.25} \right)^3 & v \in [0, \frac{1}{3}) \\ 6.3 \left( \frac{v-0.6}{0.25} \right)^5 & v \in [\frac{1}{3}, \frac{3}{4}) \\ -28 \left( \frac{v-1}{0.5} \right)^2 \cos(\frac{\pi}{2}u) & v \in [\frac{3}{4}, 1] \end{cases}$$

and

$$\beta_2^{\text{LNS}}(u, v) = \begin{cases} -20v^2 \cos(2\pi(2u-1)(2v-1)) & v \in [0, \frac{1}{2}) \\ (2-3v)^2 & v \in [\frac{1}{2}, 1] \end{cases}$$

- Nonlinear smooth (NLS): The regression model is

$$\mathcal{Y} = \Delta \left( \langle \Phi_1(\mathcal{X}^{(1)}), \beta_1^{\text{LS}} \rangle + \langle \Phi_2(\mathcal{X}^{(2)}), \beta_2^{\text{LS}} \rangle \right) + \epsilon,$$

with the following nonlinear operators

$$\Phi_1(\mathcal{X})(s) = \exp \left\{ \frac{1}{2} (1 - \mathcal{X}(s)^2) \right\}$$

and

$$\Phi_2(\mathcal{X})(s) = 1 + \frac{\mathcal{X}(s)^2}{5} + \cos(2\pi(\mathcal{X}(s)/2 - 1)) \sin(2\pi(\mathcal{X}(s)/2 - 1)).$$

- Nonlinear non-smooth (NLNS): The regression model is

$$\mathcal{Y} = \Delta \left( \langle \Phi_1(\mathcal{X}^{(1)}), \beta_1^{\text{LNS}} \rangle + \langle \Phi_2(\mathcal{X}^{(2)}), \beta_2^{\text{LNS}} \rangle \right) + \epsilon.$$

The only difference of the alternative four scenarios with just one covariate is that we only include the first term (with  $\mathcal{X}^{(1)}$ ) in the above models. In all cases, the error process  $\epsilon$  is generated on an equispaced grid of 71 points in  $[0, 1]$  from a zero-mean Gaussian process with a covariance operator available by Equation (8), where  $\sigma^2 = 0.5$ ,  $\theta = 0.3$ , and  $\Delta = 1/71$ . In order to control

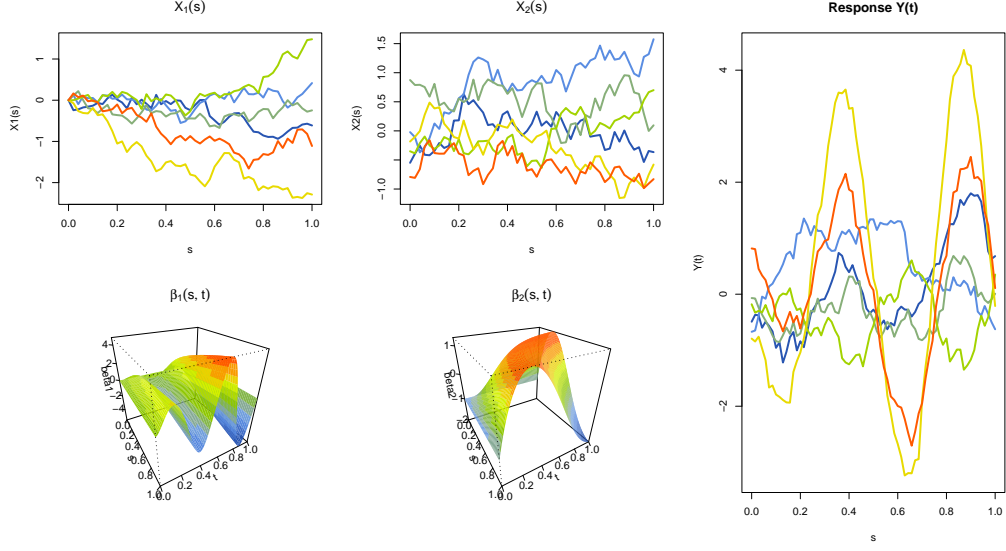


Figure 1: A sample of six realizations of the covariates and its responses jointly with the parameters for scenario 1 (Linear smooth).

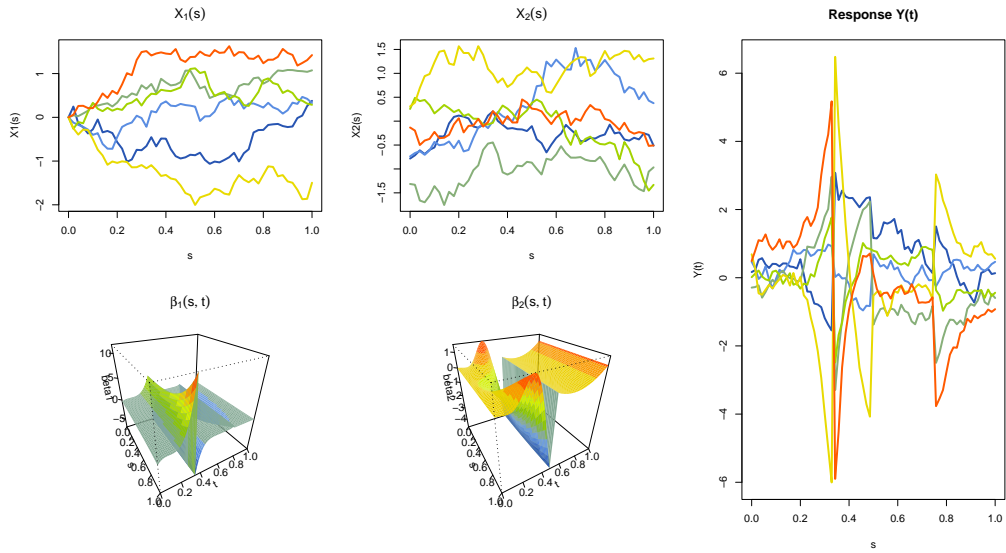


Figure 2: A sample of six realizations of the covariates and its responses jointly with the parameters for scenario 2 (Linear non-smooth).

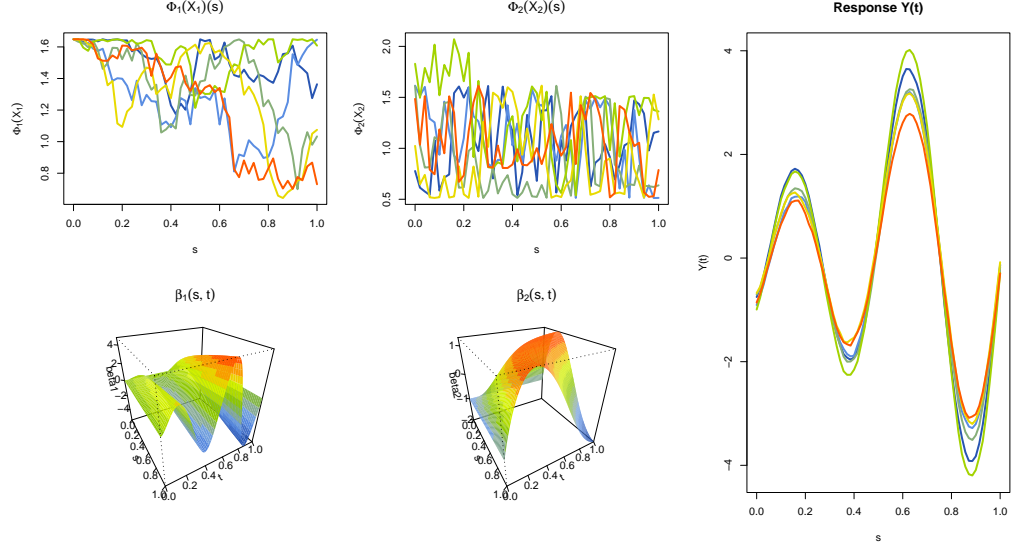


Figure 3: A sample of six realizations of the transformations of the covariates and its response jointly with the parameters for scenario 3 (Nonlinear smooth).

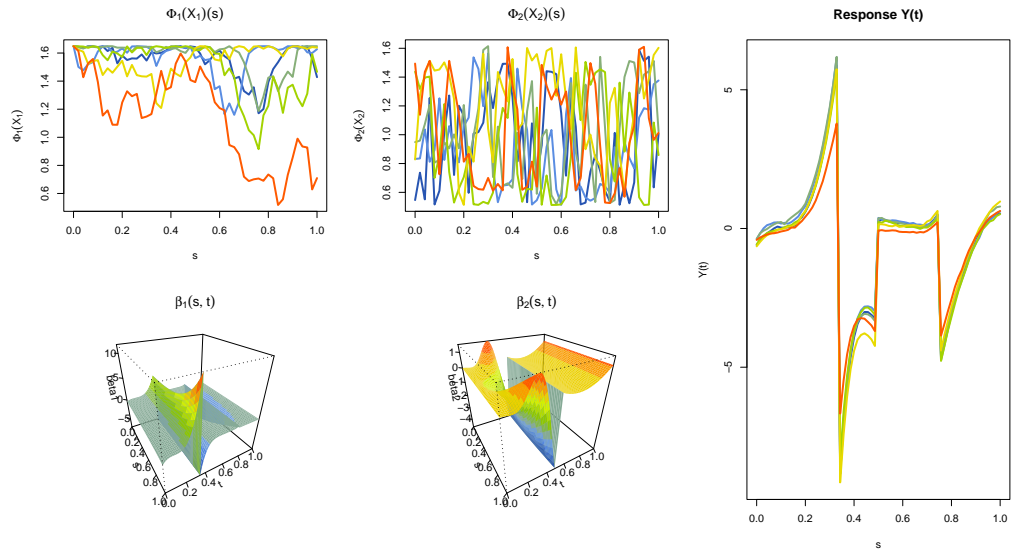


Figure 4: A sample of six realizations of the transformations of the covariates and the response jointly with the parameters for scenario 4 (Nonlinear non-smooth).

the signal-noise ratio, the  $\epsilon$  process is re-scaled to set  $\rho^2 = 0.8$ . To achieve this correlation, each error trajectory is multiplied by

$$C_\rho = \sqrt{\frac{1 - \rho^2}{\rho^2} \frac{\sum_i \|M_i - \bar{M}\|^2}{\sum_i \|\epsilon_i\|^2}},$$

where  $M_i := m(\mathcal{X}_i^{(1)}, \mathcal{X}_i^{(2)})$  is the signal (conditional expectation given covariates).

Scenarios LS (Figure 1) and NLS (Figure 3) are considered “smooth” in the sense that all the parameters and transformations involved are fairly smooth. On the other hand, scenarios LNS (Figure 2) and NLNS (Figure 4) use some parameters that are discontinuous in some null-measure subsets of their domains. It seems quite “non-smooth” for the methods based on representing all the involved functions on a smooth basis like B-splines.

Table 1 shows the results for each scenario, with two samples sizes ( $n \in \{100, 200\}$ ) and with one or two covariates (column cov.). The rows beginning with  $R_e^2$  correspond to the estimation set (each cell is the average of  $n \times 100$  values) and those beginning with  $R_p^2$  correspond to the prediction set (each cell is the mean of  $n_p \times 100 = 10000$  values).

The results for the Linear smooth scenario are expected for all methods except FAMM even though we have tried its application using different options. The table shows the results for `splinepars=list(bs="ps", k=c(31,11), m=2))`, which seems to be flexible enough. The other methods obtain values close to the nominal level of  $\rho^2 = 0.8$  with a little tendency of FSAMFR and FKAMFR to overfitting that can also be seen as a certain underestimation in the prediction set. This behavior can be motivated by two reasons: First, the estimation with these two methods can be excessively flexible and some restrictions should be applied and second, by a kind of frontier effect that in functional variates corresponds with trajectories in the prediction set far from the center. Also, by this when the sample size is incremented, the effect is lowered. The winners in this scenario are the LSC and DISC methods closely followed by PFR and FLMFR taking into account the estimation and the prediction results.

The results for Linear non-smooth scenario are clearly bad for PFR, and not so good for LSC and DISC. Recall that these methods are strongly based on representing the intermediate functions in a B-spline basis and the  $\beta$  parameters of this scenario have discontinuities for certain lines (in any case, belonging to  $\mathcal{L}_2(S) \times \mathcal{L}_2(T)$ ). The FLMFR method using PC basis is clearly the best one in this scenario although FSAMFR and FKAMFR are quite close.

In the nonlinear scenarios the methods FLMFR, PFR and LSC fail as expected. Among the nonlinear methods and excluding FAMM, DISC seems to be the winner in the nonlinear smooth scenario but fails in the non-smooth one where only the FSAMFR and FKAMFR achieve similar values to nominal in the estimation set. In any case, there is an important loss in the prediction level. The extremely negative values in nonlinear non-smooth case are due to the smoothed predictions in the neighborhood of the discontinuities of the response (see Figure 4) from FAMM, LSC and DISC methods.



Linear smooth								
$n = 100$								
	cov.	FLMFR	FSAMFR	FKAMFR	PFR	FAMM	LSC	DISC
$R_e^2$	1	0.818	0.854	0.845	0.811	0.275	0.806	0.806
$R_p^2$	1	0.781	0.741	0.768	0.776	0.188	0.793	0.793
$R_e^2$	2	0.818	0.857	0.844	0.812	0.321	0.810	0.807
$R_p^2$	2	0.781	0.735	0.750	0.776	0.223	0.787	0.782
$n = 200$								
$R_e^2$	1	0.808	0.826	0.838	0.802	0.258	0.802	0.802
$R_p^2$	1	0.793	0.780	0.781	0.787	0.222	0.799	0.799
$R_e^2$	2	0.809	0.826	0.837	0.803	0.302	0.805	0.804
$R_p^2$	2	0.792	0.779	0.768	0.787	0.264	0.794	0.791
Linear non-smooth								
$n = 100$								
	cov.	FLMFR	FSAMFR	FKAMFR	PFR	FAMM	LSC	DISC
$R_e^2$	1	0.810	0.846	0.848	0.236	0.116	0.707	0.702
$R_p^2$	1	0.780	0.742	0.764	0.218	0.052	0.696	0.691
$R_e^2$	2	0.810	0.839	0.844	0.348	0.212	0.733	0.726
$R_p^2$	2	0.783	0.753	0.743	0.322	0.141	0.717	0.713
$n = 200$								
$R_e^2$	1	0.802	0.818	0.841	0.232	0.102	0.705	0.705
$R_p^2$	1	0.782	0.770	0.772	0.223	0.073	0.696	0.695
$R_e^2$	2	0.801	0.816	0.839	0.341	0.195	0.729	0.726
$R_p^2$	2	0.786	0.776	0.758	0.333	0.163	0.720	0.718
Nonlinear smooth								
$n = 100$								
	cov.	FLMFR	FSAMFR	FKAMFR	PFR	FAMM	LSC	DISC
$R_e^2$	1	0.099	0.841	0.867	0.096	0.279	0.055	0.808
$R_p^2$	1	-0.089	0.727	0.725	-0.077	0.168	-0.049	0.781
$R_e^2$	2	0.098	0.825	0.847	0.096	0.292	0.052	0.781
$R_p^2$	2	-0.105	0.685	0.693	-0.090	0.152	-0.052	0.748
$n = 200$								
$R_e^2$	1	0.051	0.817	0.858	0.050	0.260	0.031	0.805
$R_p^2$	1	-0.058	0.763	0.751	-0.051	0.213	-0.033	0.788
$R_e^2$	2	0.049	0.795	0.838	0.049	0.268	0.027	0.779
$R_p^2$	2	-0.043	0.736	0.723	-0.037	0.208	-0.023	0.761
Nonlinear non-smooth								
$n = 100$								
	cov.	FLMFR	FSAMFR	FKAMFR	PFR	FAMM	LSC	DISC
$R_e^2$	1	0.102	0.831	0.873	-10.717	-10.656	-3.995	-3.358
$R_p^2$	1	-0.099	0.703	0.722	-10.268	-10.205	-3.919	-3.194
$R_e^2$	2	0.095	0.789	0.810	-9.611	-9.538	-3.573	-2.942
$R_p^2$	2	-0.099	0.623	0.624	-9.642	-9.574	-3.661	-3.015
$n = 200$								
$R_e^2$	1	0.051	0.803	0.858	-10.393	-10.314	-3.901	-3.225
$R_p^2$	1	-0.056	0.733	0.740	-10.387	-10.310	-3.944	-3.241
$R_e^2$	2	0.051	0.754	0.808	-9.495	-9.408	-3.546	-2.877
$R_p^2$	2	-0.051	0.681	0.667	-9.342	-9.256	-3.534	-2.870

Table 1: Simulation results ( $R_e^2$  and  $R_p^2$ ) for scenarios 1-4.

## 6 Real Data Applications

In this section, we consider two real data applications to examine the performance of all competitor methods. A third example is available in the supplementary material.

### 6.1 Bike-sharing Data

To illustrate how our proposed function-on-function methods work, we use the Bike-sharing data (Fanaee-T and Gama (2014)) as our first example. This dataset is collected by Capital Bikeshare System (CBS), Washington D.C., USA. The number of casual bike rentals (**NCR**) is considered as our functional response, and Temperature (**T**), Humidity (**H**), Wind Speed (**WS**) and Feeling Temperature (**FT**), are the functional covariates. These variables are recorded each hour from January 1<sup>st</sup>, 2011, to December 1<sup>st</sup>, 2012. Similar to Kim et al. (2018), we only consider the data for Saturday trajectories, and **NCR** is log-transformed to avoid its natural heteroskedasticity. Ignoring three curves with missing values, the dataset contains 102 trajectories, each with 24 data points (hourly) for all variables. The corresponding plots are displayed in Figure 5. Table 2 contains the distance correlation between all variables. It reveals that **FT** has the highest distance correlation with the response ( $\log(\mathbf{NCR})$ ).

Distance correlation					
	<b>NCR</b>	$\log(\mathbf{NCR} + 1)$	<b>T</b>	<b>H</b>	<b>WS</b>
<b>T</b>	0.527	0.678			
<b>H</b>	0.067	0.069	0.054		
<b>WS</b>	0.062	0.102	0.057	0.053	
<b>FT</b>	0.552	0.705	0.994	0.054	0.060

Table 2: Distance correlation among functional variables in Bike-sharing data.

Based on these values, a variable selection algorithm is performed similar to the one proposed by Febrero-Bande et al. (2019), and the covariates **FT**, **H** and **WS** were selected as relevant for the response (in that order). Note that the selection algorithm does not select **T** due to its collinearity/concurvity with **FT** (dCor:0.994). The observations are randomly split into train and test sets (82 observations are considered for the train set, and the remaining 20 are allocated to the test set). We repeat this procedure 20 times and compute the  $R_p^2$  for each one. Table 3 shows the results for the aforementioned methods once, including the submodels in order of their relevance. The median of  $R_p^2$  is shown instead of the mean as FAMM fails to converge in some cases (2–4 repetitions) due to numerical instabilities.

Table 3 reveals that whether we include all the covariates or only a subset of them, nonlinear methods provide better prediction performance than linear methods. However, the differences between the two groups are slight. With **FT**, all methods achieve a certain level that is slightly modified when we add more covariates. The addition of covariates slightly improves the  $R_p^2$  for FKAMFR and DISC. It also slightly disimproves the remaining methods. The behaviour

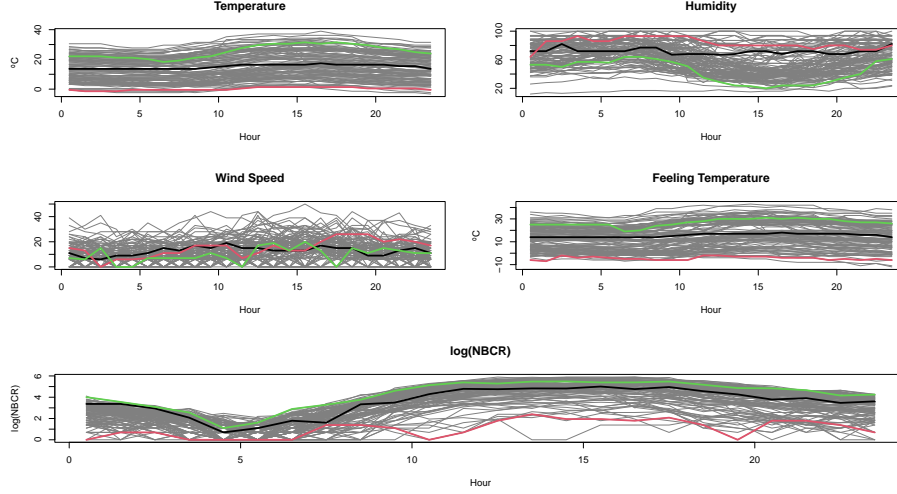


Figure 5: The plot of Bike-sharing variables over 112 Saturdays from January 1<sup>st</sup>, 2011 to December 1<sup>st</sup>, 2012. The black, red, and green lines correspond to dates September 17<sup>th</sup>, 2011, January 21<sup>st</sup>, 2012, and January 9<sup>th</sup>, 2012, respectively.

$\mathcal{Y} = \log(\mathbf{NBCR} + 1)$							
covariates	FLMFR	FSAMFR	FKAMFR	PFR	FAMM	LSC	DISC
<b>FT</b>	0.550	<b>0.621</b>	0.609	0.543	0.398	0.544	0.592
<b>FT, H</b>	0.502	0.608	<b>0.636</b>	0.512	0.510	0.486	<b>0.636</b>
<b>FT, H, WS</b>	0.522	0.560	0.644	0.507	0.561	0.500	<b>0.652</b>

Table 3: Median of  $R_p^2$  for the methods (including the covariates in order of importance) for predicting  $\log(\mathbf{NBCR} + 1)$ . The highest values per row are printed in bold.

of FAMM is an exception. It shows an increasing trend but begins with the lowest result for the model with one covariate. The slight improvement from one to two or from two to three covariates suggests that the inclusion of the third covariate (**WS**) adds more uncertainty to estimation than prediction power.

An important issue that deserves a detailed discussion is the computational cost. In this example, when needed, **FT** is represented in two PCs, **H** in four PCs, and **WS** in six PCs to ensure at least 95% of the variability of each covariate is explained. The response needs six PCs to explain 90% of the variability. These parameters are related to the complexity that can be derived from the trace of the hat matrix  $H$  ( $\hat{\mathcal{Y}} = H\mathcal{Y}$ ). For instance, in FLMFR, each covariate consumes degrees of freedom equal to the number of PCs employed. In the case of FSAMFR, the consumed degrees of freedom is  $\sum_{j=1}^{n_{PCs}} k_j$  where  $k_j$  is the complexity of the function associated with the  $j^{\text{th}}$  PC (by default up to eight). Specifically, in this example,  $k_j$  is limited to five to have fewer parameters than the number of data. The effect on the complexity of PFR, FAMM, LSC, and DISC due to the number of PC of the covariates is not apparent. The reason is that, internally, these methods represent the information on a B-spline basis. Therefore, it seems that the complexity is mainly related to the length of the B-spline basis plus some penalizing factors like in the linear methods, PFR, and LSC. In the nonlinear methods, FAMM and DISC, this effect cannot be deduced more simply, and the help of these packages does not provide further information. The complexity of FKAMFR is derived from the bandwidth values associated with each covariate, and it does not depend on the PC representation of the covariates. Regarding computational time<sup>2</sup>, FLMFR, FSAMFR, LSC, and DISC obtain times measured in milliseconds (51.5, 266.2, 112.9, 559.5, respectively), with important differences among them. PFR extends to 5.47 seconds, and FKAMFR needs 27.32 seconds, mostly employed in computing the optimal bandwidths and on the cycles of the backfitting algorithm. Finally, FAMM extends its time to 489.7 seconds without a clear reason. Recall that the use of nonlinear contributions with command `sff` is considered an experimental feature by its authors.

## 6.2 Electricity Demand and Price Data

Another interesting example comes from the Iberian Energy Market. Specifically, the daily profiles of Electricity Price ( $\mathbf{Pr}_d$ ) and Demand ( $\mathbf{En}_d$ ) (the index refers to a day), both measured hourly, are obtained from two biannual periods separated by ten years: 2008-2009 and 2018-2019 (source: [omie.es](http://omie.es)). [Febrero-Bande et al. \(2019\)](#) also employ this data, but they use a different period and focus on variable selection for scalar responses. Comparing the two periods, the profiles (see Figure 6) show a considerable reduction in demand but not a considerable price reduction.

In this example, a possible linear relationship among these two covariates is explored ( $\mathbf{Pr}_d$  explained by  $\mathbf{En}_d$ ) via a simulation study. In the simulation, we use 100 repetitions, where each period is randomly split into a training and a prediction subset (75%-25%). All the models

---

<sup>2</sup>All computational times were obtained using the package `microbenchmark`.

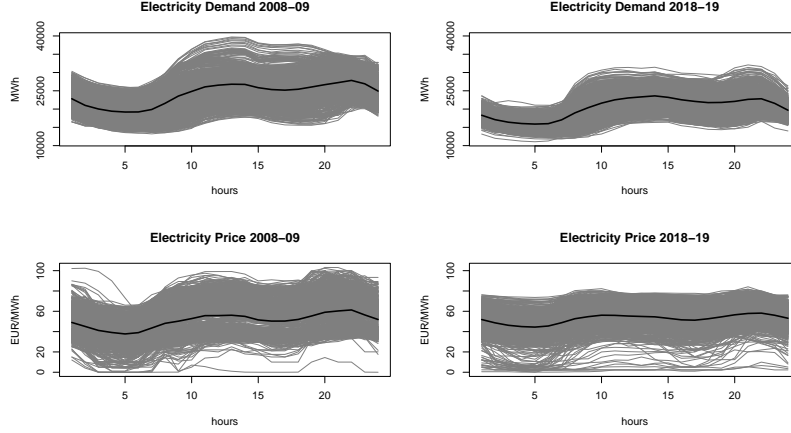


Figure 6: Profiles for Electricity Demand (first row) and Electricity Price (second row) for the periods 2008-09 (first column) and 2018-19 (second column). The black line corresponds to the functional mean of each dataset.

$\mathcal{Y} = \mathbf{Pr}_d \sim \mathbf{En}_d$							
$\bar{R}_p^2$	FLMFR	FSAMFR	FKAMFR	PFR	FAMM	LSC	DISC
2008-09	0.321	0.428	<b>0.660</b>	0.306	0.460	0.473	0.576
2018-19	0.143	0.194	<b>0.262</b>	0.137	0.161	0.197	0.201

Table 4: Mean of  $R_p^2$  for the Energy data. Periods: 2008-09 and 2018-19.

described above with only one covariate are applied to the training sample, and  $R_p^2$  is computed from the prediction sample for impartial comparative purposes. When necessary, four principal components were employed for representing  $\mathbf{Pr}$  and  $\mathbf{En}$  (more than 95% of explained variability is obtained in both cases). The results of the 100 repetitions are shown in Table 4 and Figure 7, where a significant difference between the two periods is observed. The FKAMFR method obtains the best result in both cases, with the best result of 0.660 for 2008-09. The other nonlinear methods obtain 0.576 (DISC), 0.473 (FAMM) and 0.428 (FSAMFR). These differences between nonlinear methods suggest that the nonlinearity is due to some clusters owing to different patterns for groups of days (perhaps the differences among labour and weekend days). The linear methods obtain results between 0.473 (LSC) and 0.306 (PFR), suggesting that, in this example, there is a clear nonlinear relationship among  $\mathbf{Pr}_d$  and  $\mathbf{En}_d$ . The conclusions for the second period are completely different. See the boxplots in Figure 7, which are drawn at the same scale. The numerical results are between 0.262 (FKAMFR) and 0.137 (PFR), suggesting a weak linear relationship among covariates. As in this case, we have only one covariate. Therefore, we applied the test of linearity between a single functional covariate and a functional response described by [García-Portugués et al. \(2021\)](#). For both periods, we obtain zero  $p$ -values and thus, we reject the linear hypothesis. Note that the test statistic for 2018-19 is relatively closer to the accepting region than 2008-09.

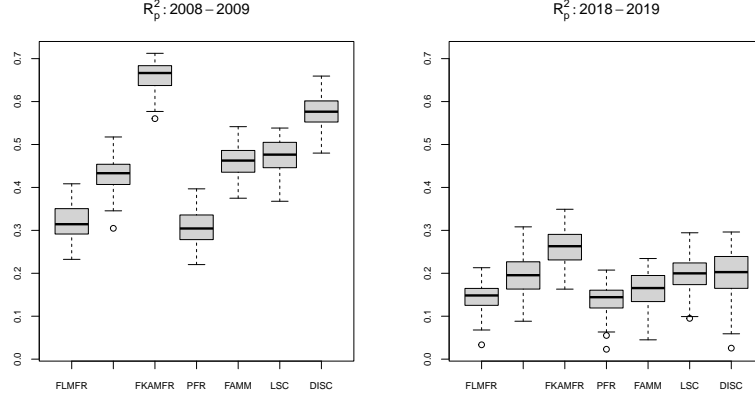


Figure 7: Boxplots for  $R_p^2$  (100 repetitions) for two different periods: 2008-2009 (left panel) and 2018-2019 (right panel).

$\mathcal{Y} = \mathbf{Pr}_d$							
$\bar{R}_p^2$	FLMFR	FSAMFR	FKAMFR	PFR	FAMM	LSC	DISC
$\mathbf{En}_{d-1}, \mathbf{En}_{d-7}$	0.336	0.456	0.631	0.324	0.564	0.600	<b>0.655</b>
$\mathbf{Pr}_{d-1}, \mathbf{Pr}_{d-7}$	<b>0.900</b>	0.881	0.886	0.886	0.859	0.898	0.881

Table 5: Average of  $R_p^2$  for prediction models with response  $\mathbf{Pr}_d$ . Period: 2008-09.

The relevant covariates for constructing predictive models (using information up to  $d - 1$  to explain  $d$ ) selected in [Febrero-Bande et al. \(2019\)](#) include mainly the lagged functional covariates at  $d - 1$  and  $d - 7$ . Following the same idea, we implement a simpler numerical study (10 repetitions) to explain  $\mathbf{Pr}_d$  with covariates  $\mathbf{En}_{d-1}, \mathbf{En}_{d-7}$  and with  $\mathbf{Pr}_{d-1}, \mathbf{Pr}_{d-7}$  using only the period 2008-09. Again, we split the data into training and prediction samples (75%-25%) with 543 curves in the training and 181 in the prediction sample. Table 5 summarizes the results. The first row (covariates  $\mathbf{En}_{d-1}, \mathbf{En}_{d-7}$ ) is similar to Table 4 but with a rise of about 0.1 for FAMM, LSC and DISC. These methods now being closer to FKAMFR and with a clear gap compared with linear methods. When the covariates are  $\mathbf{Pr}_{d-1}$  and  $\mathbf{Pr}_{d-7}$  (second row), the model seems linear because all models obtain almost the same high results (around 0.88), FLMFR being the best. This suggests that  $\mathbf{Pr}_d$  follows a persistent process, where the tomorrow price is almost perfectly explained with the today and the last week's price. In any case, the gap among the rows of Table 5 suggests that there are other factors more important than the load/demand for determining the electricity prices.

Another important factor to take into account is the computational time. FLMFR and FSAMFR take about three seconds, while PFR, LSC, and DISC need 10 to 18 seconds. FAMM and FKAMFR go over two minutes to complete their computations.

## 7 Concluding Remarks

In this paper, a review about functional regression models with functional response was provided jointly with two new nonlinear proposals: FSAMFR and FKAMFR. Both are extensions of functional regression models with scalar response and the main difference among them is the nature of the functional spaces associated with the response and the covariates. As FSAMFR is based on the representation of all functional information in bases, this proposal is restricted to be applied when the response and the covariates spaces are Hilbert. On the other hand, the estimation of a FKAMFR model mimics usual kernel regression models but using distances allowing to be applied to general metric or normed spaces. The new proposals have been implemented in both functions that will be available in next version of package `fda.usc` (the present implementation is provided in the supplementary material with the package `fda.usc.devel`). Also, a new implementation of a functional linear regression model (FLMFR) is provided that, on the contrary to previous approaches, does not need to assume that the trajectories are smooth. The previous approaches, linear (PFR and LSC) or nonlinear (FAMM and DISC), always represent the estimates using a B-spline basis that can have difficulties in scenarios with discrete discontinuities (see, for instance, scenario 2 in simulation study). These previous approaches are not similar respect to its availability. The performance of the methods included in `FRegSigCom` (LSC and DISC) is competitive but the development of the package seems to be discontinued and only old versions can be installed. The `refund` package (PFR and FAMM) has a continuous development and the performance of PFR seems reasonable when the trajectories are quite smooth. On the contrary, in our simulation scenarios, the application of FAMM, particularly with several functional covariates, was unable to obtain similar results than the other methods even though several combinations of the parameters have been tried.

## Acknowledgments

The research by Manuel Febrero-Bande and Manuel Oviedo-de la Fuente has been partially supported by the Spanish Grant PID2020-116587GB-I00 funded by MCIN/AEI/10.13039/501100011033. Indeed, Manuel Oviedo-de la Fuente has been partially supported by Spanish MINECO grant PID2020-113578RB-I00 and MTM2017-82724-R and by the Xunta de Galicia (Grupos de Referencia Competitiva ED431C-2020-14 and Centro de Investigación del Sistema universitario de Galicia ED431G 2019/01), all of them through the European Regional Development Funds (ERDF). The reseach by Mohammad Darbalaei and Morteza Amini is based upon research funded by Iran National Science Foundation (INSF) under project No. 99014748.

## References

Aneiros-Pérez, G. and Vieu, P. (2006). Semi-functional partial linear regression. *Statistics & Probability Letters*, 76(11):1102–1110.

- Beyaztas, U. and Shang, H. L. (2020). On function-on-function regression: partial least squares approach. *Environmental and Ecological Statistics*, 27(1):95–114.
- Cardot, H., Ferraty, F., and Sarda, P. (1999). Functional linear model. *Statistics & Probability Letters*, 45(1):11–22.
- Cardot, H., Ferraty, F., and Sarda, P. (2003). Spline estimators for the functional linear model. *Statistica Sinica*, 13(3):571–592.
- Cardot, H., Mas, A., and Sarda, P. (2007). Clt in functional linear regression models. *Probability Theory and Related Fields*, 138(3):325–361.
- Chen, D., Hall, P., and Müller, H. (2011). Single and multiple index functional regression models with nonparametric link. *Annals of Statistics*, 39(3):1720–1747.
- Chiou, J.-M., Müller, H.-G., and Wang, J.-L. (2003). Functional quasi-likelihood regression models with smooth random effects. *Journal of the Royal Statistical Society: Series B (Statistical Methodology)*, 65(2):405–423.
- Chiou, J.-M., Yang, Y.-F., and Chen, Y.-T. (2016). Multivariate functional linear regression and prediction. *Journal of Multivariate Analysis*, 146:301–312.
- Cuevas, A., Febrero, M., and Fraiman, R. (2002). Linear functional regression: the case of fixed design and functional response. *Canadian Journal of Statistics*, 30(2):285–300.
- Delaigle, A., Hall, P., et al. (2012). Methodology and theory for partial least squares applied to functional data. *The Annals of Statistics*, 40(1):322–352.
- Fan, Y. and James, G. (2011). Functional additive regression. Technical report, Tech. rep., Marshall School of Business, University of Southern California.
- Fanaee-T, H. and Gama, J. (2014). Event labeling combining ensemble detectors and background knowledge. *Progress in Artificial Intelligence*, 2(2):113–127.
- Febrero-Bande, M., Galeano, P., and González-Manteiga, W. (2017). Functional principal component regression and functional partial least-squares regression: An overview and a comparative study. *International Statistical Review*, 85(1):61–83.
- Febrero-Bande, M. and González-Manteiga, W. (2013). Generalized additive models for functional data. *TEST*, 22(2):278–292.
- Febrero-Bande, M., González-Manteiga, W., and de la Fuente, M. O. (2019). Variable selection in functional additive regression models. *Computational Statistics*, 34(2):469–487.
- Ferraty, F., Goia, A., Salinelli, E., and Vieu, P. (2013). Functional projection pursuit regression. *TEST*, 22(2):293–320.



- Ferraty, F., González-Manteiga, W., Martínez-Calvo, A., and Vieu, P. (2012a). Presmoothing in functional linear regression. *Statistica Sinica*, 22(1):69–94.
- Ferraty, F., Keilegom, I. V., and Vieu, P. (2012b). Regression when both response and predictor are functions. *Journal of Multivariate Analysis*, 109:10–28.
- Ferraty, F. and Vieu, P. (2006). *Nonparametric functional data analysis: theory and practice*. Springer.
- Ferraty, F. and Vieu, P. (2009). Additive prediction and boosting for functional data. *Computational Statistics & Data Analysis*, 53(4):1400–1413.
- García-Portugués, E., Álvarez Liébana, J., Álvarez Pérez, G., and González-Manteiga, W. (2021). A goodness-of-fit test for the functional linear model with functional response. *Scandinavian Journal of Statistics. Theory and Applications*, 48(2):502–528.
- Goldsmith, J., Bobb, J., Crainiceanu, C.-M., Caffo, B., and Reich, D. (2011). Penalized functional regression. *Journal of Computational and Graphical Statistics*, 20(4):830–851.
- Hall, P., Müller, H., and Wang, J. (2006). Properties of principal component methods for functional and longitudinal data analysis. *Annals of Statistics*, 34(3):1493–1517.
- Ivanescu, A. E., Staicu, A.-M., Scheipl, F., and Greven, S. (2014). Penalized function-on-function regression. *Computational Statistics*, 30(2):539–568.
- James, G., Wang, J., and Zhu, J. (2009). Functional linear regression that’s interpretable. *Annals of Statistics*, 37(5A):2083–2108.
- Jeon, J. M., Park, B. U., and Keilegom, I. V. (2021). Additive regression for non-Euclidean responses and predictors. *The Annals of Statistics*, 49(5):2611 – 2641.
- Kim, J. S., Staicu, A.-M., Maity, A., Carroll, R. J., and Ruppert, D. (2018). Additive function-on-function regression. *Journal of Computational and Graphical Statistics*, 27(1):234–244.
- Locantore, N., Marron, J., Simpson, D., Tripoli, N., Zhang, J., Cohen, K., Boente, G., Fraiman, R., Brumback, B., Croux, C., et al. (1999). Robust principal component analysis for functional data. *Test*, 8(1):1–73.
- Luo, R. and Qi, X. (2017). Function-on-function linear regression by signal compression. *Journal of the American Statistical Association*, 112(518):690–705.
- McLean, M. W., Hooker, G., Staicu, A.-M., Scheipl, F., and Ruppert, D. (2014). Functional generalized additive models. *Journal of Computational and Graphical Statistics*, 23(1):249–269.
- Müller, H. and Yao, F. (2008). Functional additive models. *Journal of the American Statistical Association*, 103(484):1534–1544.

- Preda, C. and Saporta, G. (2005). PLS regression on a stochastic process. *Computational Statistics & Data Analysis*, 48(1):149–158.
- Preda, C. and Schiltz, J. (2011). Functional pls regression with functional response: the basis expansion approach. In *Proceedings of the 14th Applied Stochastic Models and Data Analysis Conference*, pages 1126–1133. Università di Roma La Sapienza.
- Qi, X. and Luo, R. (2019). Nonlinear function-on-function additive model with multiple predictor curves. *Statistica Sinica*, 29(2):719–739.
- Ramsay, J. and Silverman, B. (2005). *Functional Data Analysis*. Springer.
- Reiss, P. and Ogden, R. (2007). Functional principal component regression and functional partial least squares. *Journal of the American Statistical Association*, 102:984–996.
- Scheipl, F., Staicu, A.-M., and Greven, S. (2015). Functional additive mixed models. *Journal of Computational and Graphical Statistics*, 24(2):477–501.

## Supplementary Material

### A Visualization Tool about Linear-Nonlinear Relationships

In multivariate framework, it could be relatively easy to construct some diagnostic plots for assessing when the partial contribution of a covariate is linear or nonlinear. This is extremely difficult in FDA due to the high dimensionality of objects involved. Nevertheless, something can be done in the case of Hilbertian response and a single Hilbertian covariate as shown in Figures 8 and 9. In both cases, we have a matrix of plots  $7 \times 3$  where the columns corresponds with the  $j^{\text{th}}$  PC of the response ( $Y.PC_j$ ). The rows are associated with the models described in the paper. And, in each row-column combination, a map of the predicted score for the  $j^{\text{th}}$  of the response is plotted for a grid of predictor  $\mathcal{X}_0 = \mu_{\mathcal{X}} + x_{0,1}\eta_1 + x_{0,2}\eta_2$  where  $x_{0,1}$  and  $x_{0,2}$  are generated in the range of the training sample and  $\eta_1, \eta_2$  are the first two principal component of the covariate. All the plots have the same scale by columns in order to compare the different models. Also, the dotted line inside each map is the convex hull of  $x_{i,1}$  and  $x_{i,2}$  from the training sample. The comparison among models must be done inside this polygon although the data cloud is not uniformly filling that convex hull.

Figure 8 corresponds to a linear example and the maps for all models are more or less the same except perhaps for FAMM (row 5) where a different pattern is shown (it seems smoother than the others in the first PC). The map for the first PC shows a clear decreasing trend from top to bottom that is also captured by the nonlinear methods (FSAMFR, FKAMFR and DISC). For the second PC, FSAMFR and FKAMFR provide a nonlinear pattern that seems not so different from the linear models inside the convex hull polygon.

Figure 9 shows an example of a nonlinear model that, as expected, is captured by FSAMFR, FKAMFR and DISC principally in the first PC (first column). FAMM captures a smoother version of the first PC and have a different pattern to the second and third PC (possibly to compensate its estimation of the first PC). The linear models (FLMFR, PFR and LSC) show a similar pattern among them different from the pattern captured by the nonlinear models.

For several covariates, a similar tool can be done fixing the other covariates to a particular values like, for instance, its mean and creating predictor vectors in the same way as before generating a grid using the two first PC components. But, it may happen that the plot seems linear because the nonlinearity were located far from the chosen fixed point. So, when this visualization tool shows a partial linear relationship, it is not a complete warranty about that assumption.

### Air Quality Data

Our last example is the Air Quality dataset (AQI) available from the UCI machine learning repository (Qi and Luo (2019)). AQI is a popular dataset that consists of a list of five metal oxide chemical sensors embedded into an air quality multisensor device. The column names in the dataset begin with PT. The sensors are labelled as Carbon monoxide (**CO**), Non-methane hydrocarbons (**NMHC**), total Nitrogen Oxides (**NOx**), Ozone (**O3**) because it is supposed

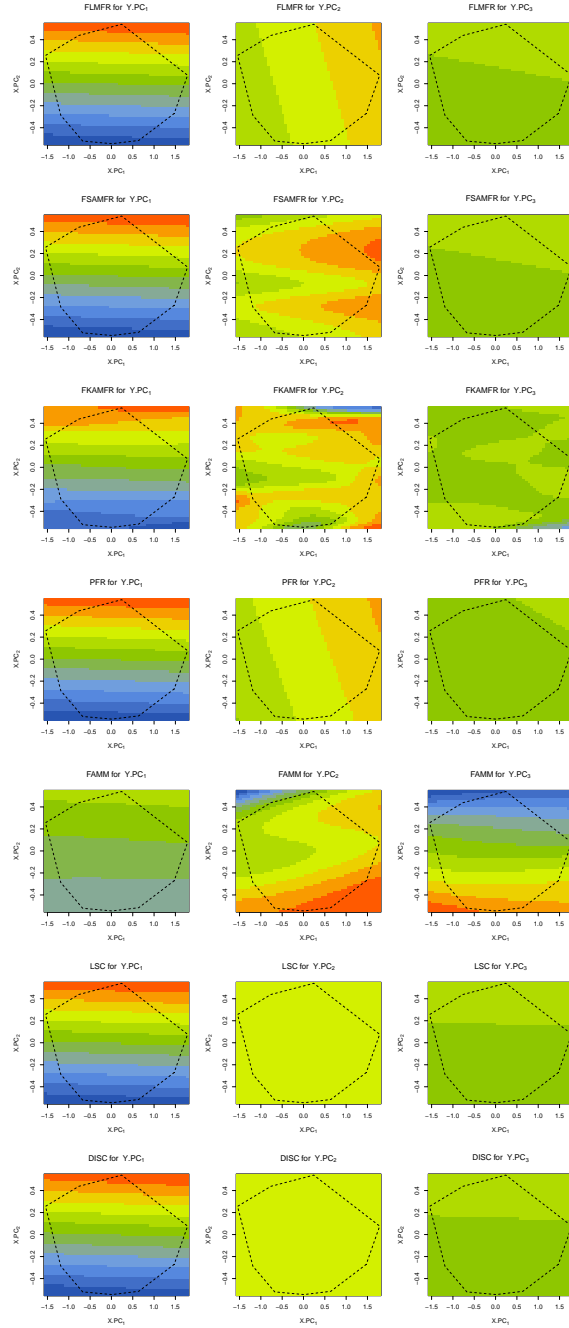


Figure 8: Maps for predictive response PC scores (by columns) as a function of the first two PC of the single covariate (Linear example). The dotted polygon inside each plot is the convex hull of the first two PCs of the covariate.

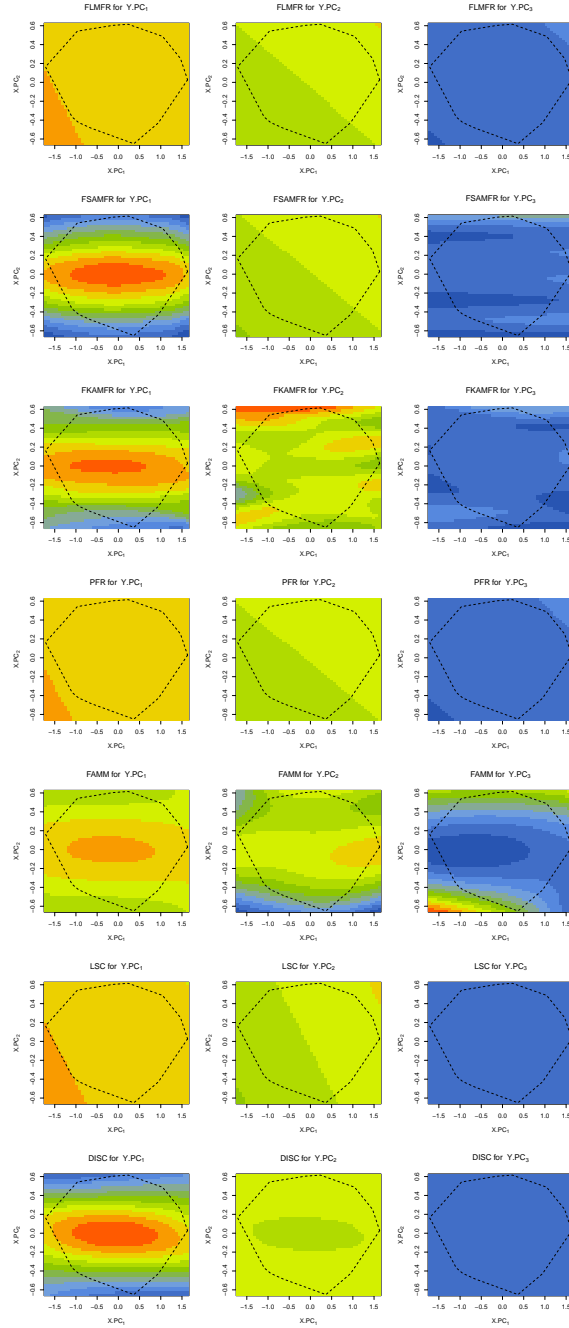


Figure 9: Maps for predictive response PC scores (by columns) as a function of the first two PC of the single covariate (Nonlinear example). The dotted polygon inside each plot is the convex hull of the first two PCs of the covariate.

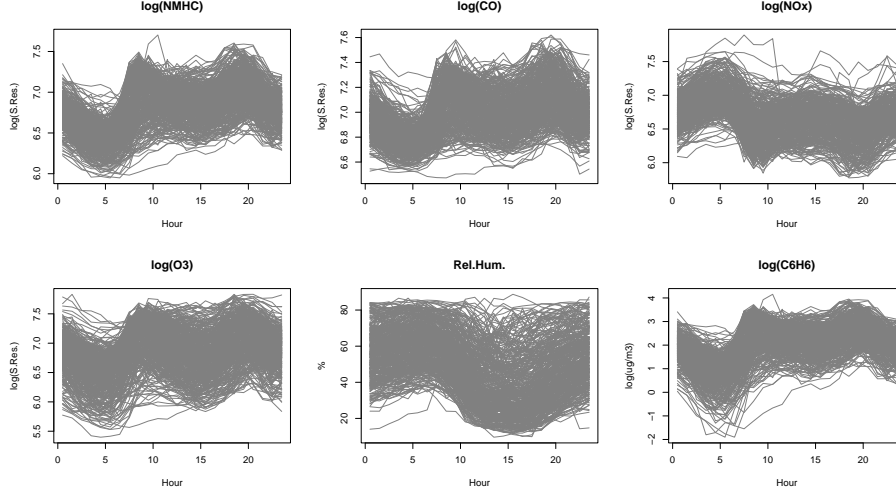


Figure 10: 355 curves for **NMHC**, **CO**, **NO<sub>x</sub>**, **O<sub>3</sub>** (obtained from sensors), and relative humidity jointly with the response **C<sub>6</sub>H<sub>6</sub>**. The signals from sensors are log-transformed.

that its measures are related with the respective pollutants. The goal of this study is to predict the content of Benzene (**C<sub>6</sub>H<sub>6</sub>**) obtained through an independent analyzer which is considered the Ground Truth. The multisensor device is placed at a road level in an Italian city during a whole year. These signals were collected as a 24 hourly averaged concentration values in each day jointly with the relative humidity (**rH**) as a external factors.

After removing the curves with missing values, we have 355 curves for each of the six functional variables shown in Figure 10. Table 6 presents the distance correlation between functional variables in the AQI dataset. We consider the curves of  $\mathcal{Y} = \ln(\mathbf{C6H6})$  as the functional response and the other five variables ( $\mathcal{X}_1 = \ln(\mathbf{NMHC})$ ,  $\mathcal{X}_2 = \ln(\mathbf{O3})$ ,  $\mathcal{X}_3 = \ln(\mathbf{CO})$ ,  $\mathcal{X}_4 = \ln(\mathbf{NOx})$  and  $\mathcal{X}_5 = \mathbf{rH}$ ) as the functional predictors.

Distance correlation					
	$\ln(\mathbf{C6H6})$	$\ln(\mathbf{NMHC})$	$\ln(\mathbf{CO})$	$\ln(\mathbf{NOx})$	$\ln(\mathbf{O3})$
$\ln(\mathbf{NMHC})$	0.986				
$\ln(\mathbf{CO})$	0.652	0.679			
$\ln(\mathbf{NOx})$	0.572	0.575	0.571		
$\ln(\mathbf{O3})$	0.791	0.800	0.782	0.683	
<b>rH</b>	0.069	0.071	0.219	0.195	0.169

Table 6: Distance correlation between functional variables in the AQI data.

To evaluate the performance of our proposed methods we randomly select 284 of the total observations as the training set and the rest of 71 as the test set. This procedure is repeated 100 times for the AQI data set, and after fitting each method on the training set, we estimate the regarding parameters for each method and then obtain the functional  $R_p^2$  for each test set. The averages of  $R_p^2$  for the 100 repetitions are tabulated in Table 7. In this table, sets M1, M2,

$\mathcal{Y} = \ln(\mathbf{C6H6})$							
Model	FLMFR	FSAMFR	FKAMFR	PFR	FAMM	LSC	DISC
M1	0.889	0.900	0.848	0.855	0.815	0.923	0.920
M2	0.892	0.901	0.858	0.864	0.817	0.926	0.912
M3	0.891	0.900	0.859	0.862	0.815	0.924	0.899

Table 7: Average of  $R_p^2$  over 100 procedures for the models (including the covariates in order of importance) for predicting  $\ln(\mathbf{C6H6})$ . M1= $\{\mathcal{X}_1\}$ , M2= $\{\mathcal{X}_1, \mathcal{X}_2, \mathcal{X}_3\}$ , and M3= $\{\mathcal{X}_1, \mathcal{X}_2, \mathcal{X}_3, \mathcal{X}_4, \mathcal{X}_5\}$ .

and M3 consider different predictors. For M1, we select only one predictor,  $\ln(\mathbf{NMHC})$ . For M2, we select three predictors:  $\ln(\mathbf{NMHC})$ ,  $\ln(\mathbf{O3})$ , and  $\ln(\mathbf{CO})$ . For M3, we use all the five predictors (namely,  $\ln(\mathbf{NMHC})$ ,  $\ln(\mathbf{O3})$ ,  $\ln(\mathbf{CO})$ ,  $\ln(\mathbf{NOx})$ , and  $\ln(\mathbf{rH})$ ). Note that we select the variables in sets M1 and M2 similar to [Febrero-Bande et al. \(2019\)](#).

The results of Table 7 reveals that the performance of linear methods are roughly the same as the nonlinear methods on all the three sets (M1, M2, M3). The simulation in the paper, also show that for the inherently linear models the performance of linear and nonlinear methods are almost the same. Thus, it seems that the function-on-function model follows a linear behavior between response and covariates on AQI. In Table 7, the results of LSC method have always shown the highest performance. With a slight difference, DISC and FSAMFR methods have the second and third best performances. Moreover, Table 7 reveals that the mentioned variable selection algorithm works well with this dataset. The reason is that in all the seven methods, increasing the number of model predictors, does not improve the performances considerably.

## Supplementary Codes and Data

- `Simulation4CesgaS.R`: Code for main simulation. Scenarios 1–4.
- `bike-sharing2.R`: Code for Bike-sharing data example.
- `hour.csv`: Bike-sharing data.
- `Exampleomel.R`: Code for Electricity Demand and Price example.
- `omel2008-09.rda`: Electricity data for 2008–09 period.
- `omel2018-19.rda`: Electricity data for 2018–19 period.
- `data-real-aqi.R`: Code for example Air Quality.
- `AirQualityUCI.xlsx`: Air Quality Data.
- `fda.usc.devel.2.0.4.tar.gz`: Package `fda.usc.devel` (Devel version of `fda.usc`) necessary for running the previous codes.